Oxidized Low-Density Lipoprotein Stimulates Macrophage ^{18}F-FDG Uptake via Hypoxia-Inducible Factor-1α Activation Through Nox2-Dependent Reactive Oxygen Species Generation

Su Jin Lee*[1], Cung Hoa Thien Quach*[2], Kyung-Ho Jung[2], Jin-Young Paik[2], Jin Hee Lee[2], Jin Won Park[2], and Kyung-Han Lee[2]

[1]*Department of Nuclear Medicine, Ajou University School of Medicine, Suwon, Korea; and* [2]*Department of Nuclear Medicine, Samsung Medical Center, Sungkyunkwan University School of Medicine, Seoul, Korea*

For ^{18}F-FDG PET to be widely used to monitor atherosclerosis progression and therapeutic response, it is crucial to better understand how macrophage glucose metabolism is influenced by the atherosclerotic microenvironment and to elucidate the molecular mechanisms of this response. Oxidized low-density lipoprotein (oxLDL) is a key player in atherosclerotic inflammation that promotes macrophage recruitment, activation, and foam cell formation. We thus explored the effect of oxLDL on macrophage ^{18}F-FDG uptake and investigated the underlying molecular mechanism including the roles of hypoxia-inducible factor-1α (HIF-1α) and reactive oxygen species (ROS). **Methods:** RAW264.7 macrophages were stimulated with native LDL, oxLDL, or lipopolysaccharide. Cells were assessed for ^{18}F-FDG uptake, lactate production, membrane glucose transporter 1 (GLUT1) expression, and hexokinase activity. ROS generation, Nox expression, and HIF-1α activity were also measured. **Results:** oxLDL (20 μg/mL) induced a 17.5 ± 1.7-fold increase in macrophage ^{18}F-FDG uptake by 24 h, which was accompanied by increased lactate production, membrane GLUT1 expression, and hexokinase activity. oxLDL-stimulated ^{18}F-FDG uptake was completely blocked by inhibitors of Src or phosphoinositide 3-kinase. ROS generation was increased to 262.4% ± 17.9% of controls by oxLDL, and *N*-acetyl-L-cysteine completely abrogated both oxLDL-induced ROS production and ^{18}F-FDG uptake. oxLDL increased Nox2 expression, and nicotinamide adenine dinucleotide phosphate oxidase inhibition totally blocked increased ROS generation and ^{18}F-FDG uptake by oxLDL. Finally, there was a clear ROS-dependent increase of HIF-1α accumulation by oxLDL, and silencing of HIF-1α completely abolished the metabolic effect of oxLDL. **Conclusion:** oxLDL is a strong stimulator of macrophage ^{18}F-FDG uptake and glycolysis through upregulation of GLUT1 and hexokinase. This metabolic response is mediated by Nox2-dependent ROS generation that promotes HIF-1α activation.

Key Words: oxidized LDL; macrophage; ^{18}F-FDG; PET; reactive oxygen species; HIF-1α

J Nucl Med 2014; 55:1699–1705
DOI: 10.2967/jnumed.114.139428

Received Feb. 21, 2014; revision accepted Jul. 24, 2014.
For correspondence or reprints contact: Kyung-Han Lee, Department of Nuclear Medicine, Samsung Medical Center, 50 Ilwon-dong, Gangnam-gu, Seoul, Korea.
E-mail: khnm.lee@samsung.com
*Contributed equally to this work.
Published online Sep. 11, 2014.

Atherosclerosis is an inflammatory disease in which macrophages activated through proinflammatory stimuli dynamically interact with vascular tissue to drive plaque progression (*1*). PET using ^{18}F-FDG provides noninvasive imaging of atherosclerotic plaque inflammation (*2*). In human subjects, ^{18}F-FDG uptake in atherosclerotic lesions is increased in a manner that correlates to cardiovascular risk (*3,4*) and is reduced after drug treatment or risk modification (*5,6*). Thus, ^{18}F-FDG PET holds promise for monitoring disease progression and therapeutic response. However, to realize its full clinical potential, we crucially need a better understanding of how macrophage glucose metabolism is altered by the atherosclerotic microenvironment and the precise molecular mechanisms that regulate this metabolic response.

A key promoter of atherosclerotic inflammation including monocyte recruitment (*7*), macrophage survival (*8*), activation, and foam cell formation (*9*) is a modified form of low-density lipoprotein (LDL) called oxidized LDL (oxLDL). Proinflammatory cytokines and lipopolysaccharide are effective stimulators of macrophage ^{18}F-FDG uptake (*10–12*), implicating a connection of macrophage glucose metabolism to inflammatory phenotype. Similarly, exposure to modified LDL has been shown to promote glucose metabolism of macrophages (*13–15*). High ^{18}F-FDG avidity of atherosclerotic plaques can thus be thought to reflect heightened macrophage glucose use due to an elevated energy requirement from immune activation.

However, not all studies have asserted this link. A recent study observed that macrophage glucose uptake was potently stimulated by hypoxia but not by proinflammatory cytokines (*16*), suggesting that hypoxia inducible factor-1α (HIF-1α) may have an important role for stimulating macrophage glucose metabolism in atherosclerotic lesions. Indeed, macrophages are well-adapted to oxygen-limiting microenvironments (*17*), in which they depend on HIF-1α activity to enhance glycolysis and promote their survival (*18*). HIF-1α also plays an essential role in inflammatory activation of phagocytes under normal oxygen tension (*19,20*), raising the question of whether the effect of oxLDL exposure on glucose metabolism of normoxic macrophages is a HIF-1α signaling-dependent response.

It is also of interest that macrophages treated with oxLDL can display an increase of reactive oxygen species (ROS) generation (*21*). ROS has been implicated in HIF-1α stabilization (*22–24*), and lipopolysaccharide and oxLDL have been shown to induce both ROS generation and HIF-1α activation in normoxic macrophages (*25,26*).

In this study, we thus tested the hypothesis that oxLDL stimulates macrophage ^{18}F-FDG uptake through a shift of glucose metabolism

toward glycolytic flux via a mechanism that involves ROS-mediated HIF-1α activation.

MATERIALS AND METHODS

Cell Culture

RAW 264.7 cells and J774A.1 cells were from the Korean Cell Line Bank. Peritoneal resident macrophages were prepared by injecting 5 mL of 3.8% thioglycollate medium (BD) into the peritoneum of C57BL/6 mice. Cells harvested from mice at day 3 were transferred to a culture plate, and macrophages attached to the bottom of the plates were collected 8 h later. Human monocytes were isolated from the peripheral blood of a normal healthy volunteer by centrifugation with Histopaque 1077 (Sigma). The mononuclear cell layer was collected and washed with phosphate-buffered saline (PBS). Cells were suspended in RPMI 1640 medium (Gibco BRL) supplemented with 10% fetal bovine serum and plated in 150-mm plates. After 2 h, nonadherent cells were removed by washing 3 times with RPMI medium. Maturation of monocytes to macrophages was induced by incubation in RPMI medium containing 10% autologous serum for 5 d. Cells were maintained in Dulbecco modified Eagle medium containing glucose (4.5 g/L) (Gibco BRL; RAW 264.7 cells) or RPMI 1640 medium (other cells) supplemented with 10% fetal bovine serum, 2 mM L-glutamine, and penicillin–streptomycin (100 U/mL) in 5% CO_2 at 37°C. For experiments, cells were seeded in medium containing 2% fetal bovine serum. The medium was changed 24 h later, and cells were treated with oxLDL (Academy Bio-Medical Co.), native LDL (nLDL), or vehicle.

^{18}F-FDG Uptake Measurement

Cells were incubated for 30 min in 5% CO_2 at 37°C with the glucose analog ^{18}F-FDG (370 kBq per well) added to culture medium. After rapid washing twice with cold PBS, cells were lysed with 0.1N NaOH and radioactivity was measured on a γ counter (Wallac). Results were expressed as percentage uptake relative to controls normalized to protein content.

nLDL, oxLDL, and lipopolysaccharide were added to culture medium at 24 h or indicated time points before ^{18}F-FDG uptake measurements. Blocking agents were added 2 h before initiation of oxLDL or lipopolysaccharide stimulation. These included the ROS scavenger *N*-acetyl-L-cysteine (NAC; Sigma), the nicotinamide adenine dinucleotide phosphate (NADPH) oxidase inhibitors diphenyleniodonium chloride (DPI; Sigma) and 4-(2-aminoethyl)-benzenesulfonyl fluoride (AEBSF; Sigma; 0.3 mM), the Src inhibitor PP2 (Sigma), the phosphoinositide 3-kinase (PI3K) inhibitor LY-294002 (Sigma), and the mitogen-activated protein kinase inhibitor PD-98059 (Sigma).

Sulforhodamine-B (SRB) Assay

The influence of different treatments on RAW cell viability was evaluated using SRB (Sigma) assays. In brief, cells were fixed for 1 h at 4°C in 3.3% (w/v) trichloroacetic acid (Sigma) without removing culture medium. After the plates were removed from the fixation solution and tapped to completely dry, each well of cells was incubated with 100 μL of 0.057% (w/v) SRB at room temperature for 30 min. The wells were then rinsed 4 times with 1% (v/v) acetic acid (Merck) and dried, and stained cells were dissolved in 200 μL of 10 mM Tris base (pH 10.5) for 5 min with shaking. Finally, absorbance at 510 nm was measured on a microplate reader.

Hexokinase Assay

Cell homogenates were removed of cell debris by centrifugation at 1,000*g* at 4°C for 5 min, and supernatants were transferred to new tubes and used as samples. Briefly, 50 μL of samples were added to 2.52 mL of reaction mixture containing 39 mM triethanolamine, 216 mM D-glucose, 0.74 mM adenosine 5′-triphosphate, 7.8 mM magnesium chloride, 1.1 mM β-nicotinamide adenine dinucleotide phosphate, and 2.5 units of glucose 6-phosphate dehydrogenase. Formation of the reaction product, NADPH, at 25°C was monitored by spectrophotometric measurements of increase in absorbance at 340 nm. One unit was defined as the amount of hexokinase activity that phosphorylates 1 μM D-glucose per min at 25°C. Final results were expressed as percentage of units per milligram of protein relative to that of control samples.

Lactate Production Assay

L-lactate in 100 μL of culture medium was measured using a Cobas assay kit (Roche/Hitachi) in which lactate is enzymatically converted to pyruvate and hydrogen peroxide. Hydrogen peroxide then undergoes an enzymatic reaction to generate a colored dye that is measured by absorbance on a microplate spectrophotometer, and lactate concentration is calculated in mU/mg from a standard curve of serially diluted standards.

Intracellular ROS Measurement

Intracellular ROS was measured using 5-(and-6)-chloromethyl-2′,7′-dichlorodihydrofluorescein diacetate acetyl ester (CM-H_2-DCFDA; Invitrogen), a cell-permeable dye that freely enters intact cells and is converted into fluorescent 2,7-dichlorofluorescein in the presence of oxidative substances. Briefly, cells washed with PBS were incubated with 10 μM CM-H_2-DCFDA for 30 min at 37°C. After PBS washing, fluorescent signal intensities at 490 nm excitation and 510- to 570-nm emission wavelengths were measured using a Gliomax Multi detection system (Promega).

Immunoblotting of Plasma Membrane GLUT1

Cells in 100-mm plates were washed with PBS and solubilized in 500 μL of lysis buffer containing sucrose (0.0856 g/mL), 10 mM *N*-(2-hydroxyethyl)piperazine-*N*′-(2-ethanesulfonic acid) (HEPES), 25 μM ethylenediaminetetraacetic acid, aprotinin (10 μg/mL), leupeptin (10 μg/mL), and 1 mM phenylmethylsulfonylfluoride. Cell debris was eliminated by centrifugation at 1,000*g*, and the supernatant was incubated at 4°C for 1 h with 1.5 mL of lysis buffer (sucrose [0.0856 g/mL], 10 mM HEPES, and 10 mM $MgCl_2$). After centrifugation at 45,000 rpm for 60 min, the membrane fraction pellet was dissolved in PBS and 20 μg were separated on a 10% polyacrylamide gel. The protein was transferred to lanes of a hydrobond ECL nitrocellulose membrane (Amersham Biosciences) and incubated overnight at 4°C with a polyclonal antihuman GLUT1 antibody (Abcam; 1:1,000 dilution). Immunoreactive protein was visualized by 1-h incubation with a horseradish peroxidase

TABLE 1
Reverse Transcriptase PCR Primer Sequences

Primer	Forward	Reverse
Nox1	5′ TTTCTCTCCCGAAGGACCTCT 3′	5′ TGCCACCAGCTTATGGAAGG 3′
Nox2	5′ TTTGTCAAGTGCCCCAAGGT 3′	5′ GGCATCTTGGAACTCCTGCT 3′
Nox4	5′ CAGAAGGTCCCTAGCAGGAG 3′	5′ GCTGCATTCAGTTCAAGGAA 3′

(HRP)–conjugated antirabbit IgG antibody (Cell Signaling; 1:5,000 dilution) and exposure on a high-performance chemiluminescence film.

Immunoblotting of HIF1-α and Silencing with Specific Small Interfering RNA (siRNA)

Total cell lysates were prepared using PRO-PREP protein extraction solution (iNtRON Biotechnology), followed by Bradford protein assays. An equal amount of 30 μg of protein was loaded into 8% sodium dodecyl sulfate polyacrylamide gel, separated by electrophoresis, and transferred to a nitrocellulose membrane. After blocking with 5% skim milk in Tris-buffered saline with Tween 20 for 1 h at room temperature, the membrane was incubated overnight at 4°C with a rabbit polyclonal antibody against HIF-1α (Abnova; 1:5,000 dilution). For loading control, membranes were incubated with monoclonal antibody against β-actin (Santa Cruz; 1:5,000 dilution). The membrane was then incubated with secondary antibodies at room temperature for 1 h. The secondary antibody was HRP-linked antirabbit IgG antibody for HIF-1α (Cell Signaling; 1:5,000 dilution) and HRP-linked antimouse IgG antibody for β-actin (Cell Signaling; 1:5,000 dilution).

To silence HIF-1α expression, cells on a 24-well plate were transfected with mouse specific–HIF-1α siRNA (Santa Cruz) or scramble control siRNA (Cell Signaling) using Lipofectamine LTX (Invitrogen) according to the manufacturer's protocol. Cells were used for experiments 48 h later.

Immunoblotting and Reverse Transcriptase Polymerase Chain Reaction (PCR) for Nox2 and Nox4 Expression

For immunoblotting, cells were lysed in PRO-PREP protein extraction solution (iNtRON Biotechnology). Protein (60 μg) was loaded in 10% sodium dodecyl sulfate polyacrylamide gel, separated by electrophoresis, and transferred to a nitrocellulose membrane. The membrane was incubated overnight at 4°C with goat polyclonal g91-phox/Nox2 (C-15) or Nox4 antibodies (Santa Cruz; 1:500 dilution), followed by incubation for 1 h at room temperature with donkey antigoat IgG-HRP (Santa Cruz; 1:5,000 dilution). β-actin was used as loading control.

For reverse transcriptase PCR experiments, total cellular RNA was extracted using an RNeasy kit (Qiagen), and messenger RNA (mRNA) (5 μg) was reverse-transcribed to complementary DNA using an AccuPower RocketScript Cycle RT Premix kit (Bioneer) (Table 1). Nox1, Nox2, and Nox4 mRNA levels were determined by real-time PCR using quantitative PCR PreMix (Bioneer) and an ABI 7300 system (Applied Biosystems). All data were normalized to the mRNA level of glyceraldehyde-3-phosphate dehydrogenase.

Statistical Analysis

Results are expressed as mean ± SD or mean ± SE as indicated. Significance of difference between groups was evaluated by the Student tests for 2 groups and by ANOVA with Scheffé post hoc tests for 3 or more groups. *P* values of less than 0.05 were considered significant.

RESULTS

Effect of oxLDL on Macrophage ^{18}F-FDG Uptake

RAW264.7 cells, J774A.1 cells, murine peritoneal resident macrophages, and human monocyte/macrophages all displayed augmented glucose uptake by 24 h of exposure to oxLDL. For RAW264.7 cells, ^{18}F-FDG uptake increased to 319.5 ± 68.9% of controls by 5 μg of oxLDL per milliliter (Fig. 1A). For J774A.1 cells, murine peritoneal macrophages, and human macrophages, 20 μg of oxLDL per milliliter increased ^{18}F-FDG uptake to 178.8% ± 8.9%, 144.1% ± 2.6%, and 227.2% ± 28.1% of control levels, respectively (Fig. 1A).

Further inspection in RAW264.7 cells showed that oxLDL stimulated ^{18}F-FDG uptake in a dose-dependent manner, with uptake levels reaching as high as 17.5 ± 1.7-fold of controls by a concentration of 20 μg/mL (Fig. 1B). This uptake level was greater than the 11.2 ± 0.7-fold increase achieved by 100 ng of lipopolysaccharide per milliliter (Fig. 1B). Time course experiments demonstrated that both oxLDL and lipopolysaccharide

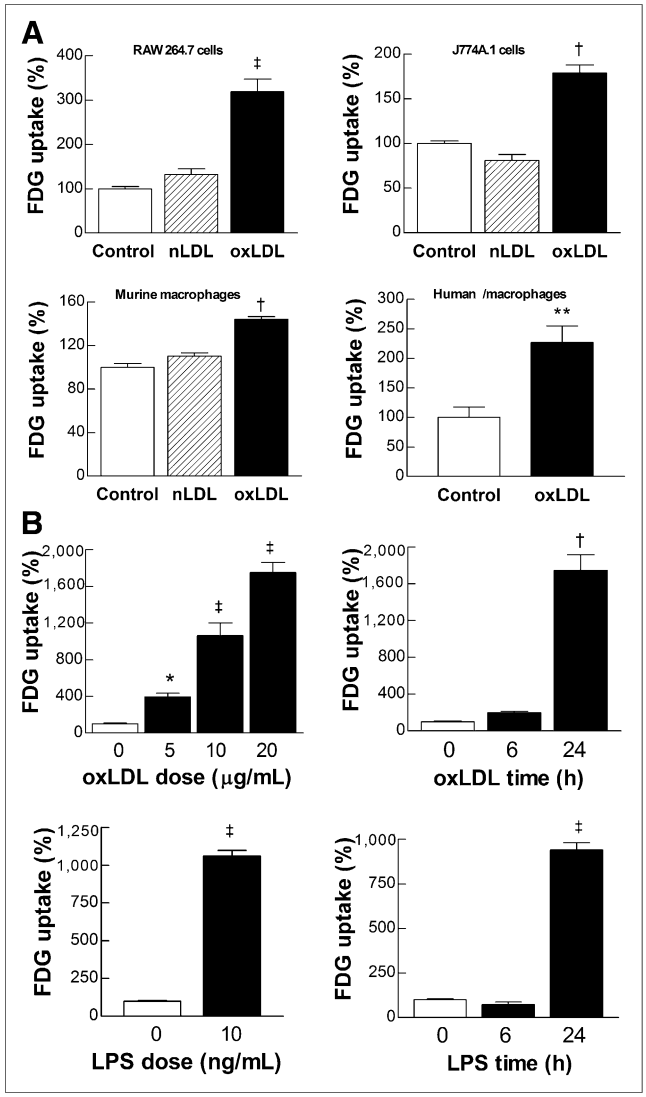

FIGURE 1. oxLDL enhances glucose uptake in macrophages. (A) RAW264.7 cells, J774A.1 cells, mouse peritoneal resident macrophages, and human peripheral monocytes/macrophages were exposed to oxLDL (5 μg/mL for RAW264.7 cells and 20 μg/mL for other cells) for 24 h and measured for 30-min ^{18}F-FDG uptake. Bars are mean ± SEM of data from 3 independent experiments (n = 6; RAW264.7 cells) or mean ± SD of duplicate samples from single experiment (other cells). (B) Dose- (left) and time-dependent (right) effects of stimulation with oxLDL (top) or lipopolysaccharide (bottom) on RAW264.7 cell ^{18}F-FDG uptake. Dose effects were performed with 24-h treatment and time effects were done with 20 μg of oxLDL per milliliter or 100 ng of lipopolysaccharide per milliliter. Bars are mean ± SD of triplicate (dose effects) or duplicate (time effects) samples from single experiment expressed as percentage uptake relative to controls. *$P < 0.05$, **$P < 0.01$, †$P < 0.0005$, and ‡$P < 0.0001$, compared with controls. LPS = lipopolysaccharide.

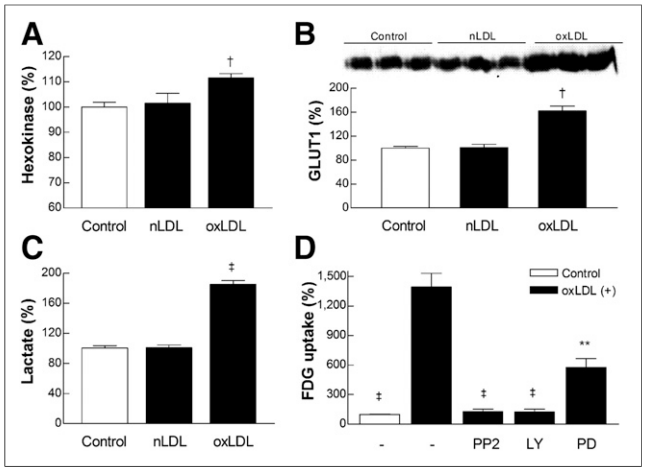

FIGURE 2. oxLDL augments macrophage glycolysis by upregulating hexokinase and GLUT1. (A) Total hexokinase activity in RAW264.7 cells treated with 20 μg of nLDL or oxLDL per milliliter for 24 h. (B) Western blots with protein band intensities for plasma membrane expressed GLUT1 levels in cells treated as above. Equivalent protein loading was confirmed by Ponceau staining of membrane, and absence of contamination by cytoplasmic protein was verified with anti–β-actin antibody. (C) Lactate production measured as concentration in medium of cells treated as above. (D) Effects of inhibitors of Src (PP2, 10 μM), PI3K (LY-294002, 5 μM), and mitogen-activated protein kinase (PD-98059, 50 μM) pathways on ^{18}F-FDG uptake in cells stimulated with oxLDL (20 μg/mL). Bars are mean ± SEM of data from 2 independent experiments ($n = 6$; A and D) or mean ± SD of triplicate samples from single experiment (B and C) expressed as percentage level relative to controls. $^{**}P < 0.01$, $^{\dagger}P < 0.0005$, and $^{\ddagger}P < 0.0001$, compared with control group (A–C) or oxLDL group (D).

required 24 h of stimulation for a full-blown effect on glucose uptake (Fig. 1B).

Glycolytic Flux, Hexokinase Activity, and GLUT1 Expression

Hexokinase and GLUT1 were investigated as 2 major regulators of cellular glucose uptake. The results showed that 24-h exposure to 20 μg of oxLDL per milliliter mildly but significantly increased RAW264.7 cell hexokinase activity (111.6% ± 3.5% of controls; Fig. 2A). Plasma membrane GLUT1 expression evaluated by Western blots was clearly increased to 161.8% ± 8.5% of controls (Fig. 2B). Lactate production was increased to 185.3% ± 4.8% of controls by 20 μg of oxLDL per milliliter (Fig. 2C), indicating augmented glycolytic flux as the major driving force for increased glucose uptake. Blocking experiments of candidate intracellular signaling pathways showed that inhibition of Src with PP2 and PI3K with LY-294002 completely blocked oxLDL-stimulated ^{18}F-FDG uptake. Inhibition of mitogen-activated protein kinase signaling with PD-98059 caused a partial suppression of the effect (Fig. 2D).

Requirement of ROS Promotion for oxLDL Effect

ROS generation in RAW264.7 cells was substantially increased to 262.4% ± 17.9% of controls by 8-h treatment with 20 μg of oxLDL per milliliter (Fig. 3A), which was comparable to that induced by 100 ng of lipopolysaccharide per milliliter (295.9% ± 20.4% of controls; Fig. 3A). nLDL did not stimulate ROS generation (Fig. 3A). Time course experiments showed that ROS production began to increase from 4 h and reached a plateau by 8 h of oxLDL treatment (Fig. 3B).

Scavenging of ROS with 10 mM NAC effectively blocked the increase of ROS generation by oxLDL as well as that by lipopolysaccharide (Supplemental Fig. 1A [supplemental materials are available at http://jnm.snmjournals.org]). This was accompanied by a complete loss of the ability of oxLDL to augment ^{18}F-FDG uptake (Supplement Fig. 1B), indicating the requirement of increased ROS production for the metabolic effect.

Involvement of NADPH Oxidase

DPI (1 μM) and AEBSF (0.3 mM) completely abrogated the effects of oxLDL and lipopolysaccharide to promote ROS generation in (Fig. 4A). Furthermore, this cancelation of effects on ROS was accompanied by a complete abolishment of oxLDL- and lipopolysaccharide-induced increase of ^{18}F-FDG uptake (Fig. 4A). To exclude the influence of altered cell viability on these results, we performed SRB assays and found that treatment with 20 μL of oxLDL per milliliter or 100 ng of lipopolysaccharide per milliliter for 24 h did not affect cell content (data not shown). Cotreatment with 20 μL of oxLDL per milliliter and 1 μM DPI or 0.3 mM AEBSF appeared to slightly decrease cell content, compared with treatment with oxLDL only, but not to a statistically significant degree (87.3% ± 8.3%, $P = 0.27$, and 80.2% ± 2.6%, $P = 0.09$, respectively). These findings indicate that the abilities of DPI and AEBSF to completely suppress oxLDL-stimulated ^{18}F-FDG uptake are not likely to have been significantly contributed to by their influence on cell viability.

oxLDL treatment significantly increased Nox2 mRNA and protein expression (Fig. 4B). In contrast, Nox4 mRNA and protein levels were undetected in RAW264.7 cells with or without oxLDL treatment (data not shown). Nox1 mRNA was also low at baseline and did not increase but rather slightly decreased by oxLDL treatment from 1.38 ± 0.09 to 1.00 ± 0.08 ($P < 0.01$; data not shown).

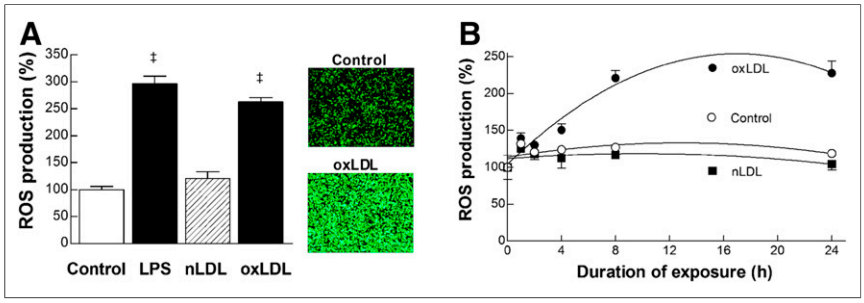

FIGURE 3. Augmented generation of ROS is required for lipopolysaccharide and oxLDL effects. (A) ROS production in RAW264.7 cells treated for 24 h with lipopolysaccharide (100 ng/mL), nLDL (20 μg/mL), or oxLDL (20 μg/mL). Data are mean ± SEM of results from 2 independent experiments ($n = 5$). $^{\ddagger}P < 0.0001$, compared with controls. Fluorescent microscopy images of cells undergoing CM-H_2-DCFDA assays as measure of intracellular ROS are shown. (B) Time course of stimulated ROS production by 20 μg of nLDL or oxLDL per milliliter. Data are mean ± SD of duplicate samples. LPS = lipopolysaccharide.

Requirement of ROS-Mediated HIF-1α Activation

RAW264.7 cells treated with oxLDL for 24 h demonstrated markedly increased levels of HIF-1α accumulation, which peaked at 6 h and persisted for up to 24 h (Fig. 5A).

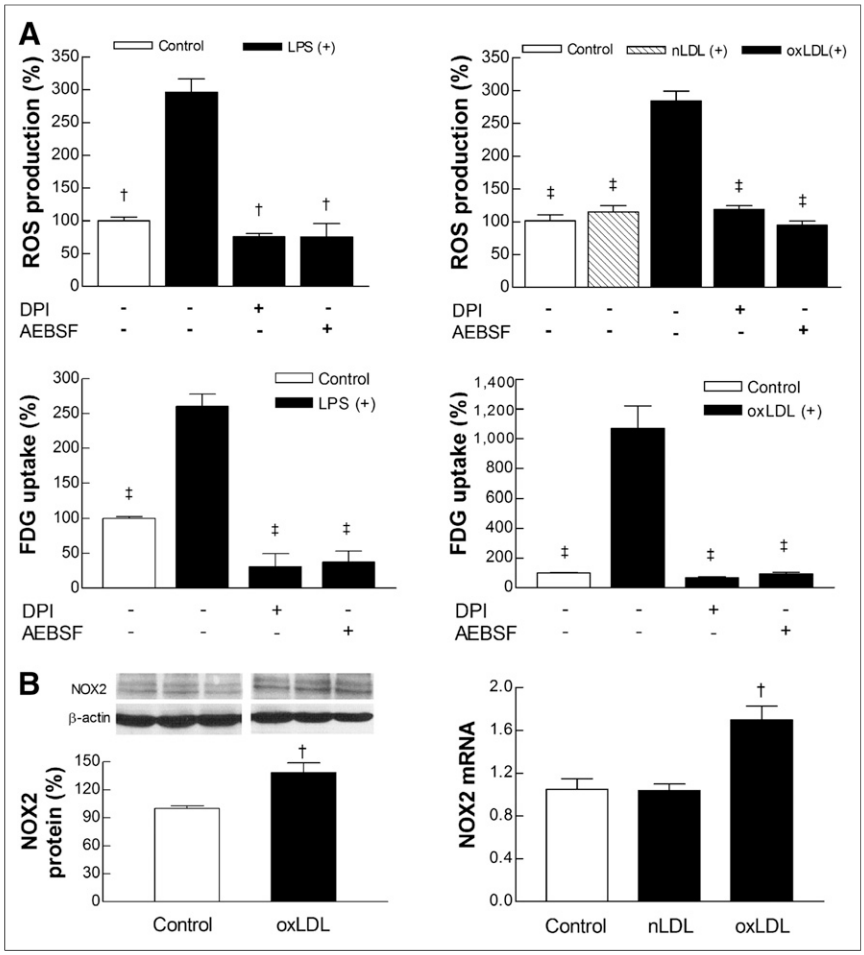

FIGURE 4. oxLDL stimulates macrophage ROS production through NADPH oxidase. (A) Effects of the NADPH oxidase inhibitors DPI (1 μM) and AEBSF (0.3 mM) on ROS generation (top) or ^{18}F-FDG uptake (bottom) stimulated by lipopolysaccharide (100 ng/mL; left) or oxLDL (20 μg/mL; right). Data are mean ± SD of duplicate samples of single experiment (lipopolysaccharide effect on ROS) or mean ± SEM of results from 2 independent experiments (remaining data). †$P < 0.0005$ and ‡$P < 0.0001$, compared with cells stimulated without inhibitors. (B) Western blots with protein band intensities (left) and mRNA levels (right) for Nox2 expression in oxLDL-stimulated RAW264.7 cells. Bars are mean ± SD of triplicate samples from single experiment (left) or mean ± SEM of data from 2 independent experiments ($n = 6$; right). †$P < 0.0005$ and ‡$P < 0.0001$, compared with controls. LPS = lipopolysaccharide.

This effect was completely abolished by NADPH oxidase inhibition with AEBSF or DPI as well as by ROS scavenging with NAC (Fig. 5B). Furthermore, silencing of HIF-1α expression with specific siRNA (Fig. 5C) was sufficient to completely block the ability of oxLDL to enhance ^{18}F-FDG uptake (Fig. 5D).

DISCUSSION

This study shows that oxLDL is a strong stimulator of ^{18}F-FDG uptake in macrophages including RAW264.7 cells, J774A.1 cells, mouse peritoneal macrophages, and human monocyte/macrophages. In RAW264.7 macrophages, this augmented uptake occurred in a dose- and time-dependent fashion and was accompanied by an elevation of lactate generation, indicating a shift of glucose metabolism toward glycolytic flux.

The increase of ^{18}F-FDG uptake induced by oxLDL was shown to be mediated through upregulation of both cell surface expression of GLUT1, the major glucose transporter subtype in macrophages (*27*), and activity of hexokinase, the first of a series of enzymes through which glucose is metabolized. On examining candidate kinase pathways, the metabolic effect of oxLDL was completely abrogated by an Src inhibitor (PP2), a critical player in the functional activation of macrophages (*28*), as well as by a PI3K inhibitor (LY-294002), consistent with the regulatory role of this pathway in glucose metabolism and immune cell activation (*29*).

Atherogenesis-associated macrophage functions can be regulated by ROS that signal through redox-sensitive proinflammatory pathways (*21*). Inflammatory macrophages are a major source of ROS found in atherosclerotic plaques, which acts as a second messenger of inflammatory response (*30*). Our assay using a redox-sensitive DCFH-DA dye revealed that oxLDL induced a substantial augmentation of ROS production paralleling the effect of lipopolysaccharide. In oxLDL-treated cells, intracellular ROS increased in a time-dependent manner and reached a plateau by 8 h. This ROS increase was a requirement for the metabolic effects of both oxLDL and lipopolysaccharide, because they were completely abolished by scavenging of ROS with NAC.

Whereas ROS can be generated by a variety of sources according to cell type, NADPH oxidases are the professional producer in phagocytic cells (*31*). Consistent with this, our results showed that inhibition of NADPH oxidase with DPI or AEBSF totally abrogated the capacity of oxLDL and lipopolysaccharide to induce ROS generation. Importantly, this was accompanied by total blocking of oxLDL- and lipopolysaccharide-stimulated ^{18}F-FDG uptake. DPI acts by abstracting an electron from an electron transporter and may nonspecifically inhibit several different electron transporters in addition to Nox isoforms. AEBSF blocks serine protease activity by interfering with cytoplasmic subunit association and could also inhibit effects unrelated to Nox. Neither DPI nor AEBSF is entirely specific for Nox, and inhibition data without additional support by specific Nox2 siRNA should be taken with some caution.

Nox2 is the prototype NADPH oxidase in macrophages that constitutes the primary source of ROS during oxidative burst (*31*). In a previous study with J774 macrophages, Nox2 was shown to mediate an increase of ROS generation stimulated by minimally oxidized LDL (*21*). In our results, oxLDL increased both Nox2 mRNA and protein levels. Although Nox4 was previously identified as a source of ROS induced by oxLDL in HMDM macrophages (*32*), we were not able to detect Nox4 mRNA or protein in RAW264.7 cells, similar to previous reports (*33*). Also consistent with previous observations (*33*), we found low Nox1 mRNA levels in RAW264.7 cells at baseline. Furthermore, Nox1 mRNA did not increase after oxLDL stimulation.

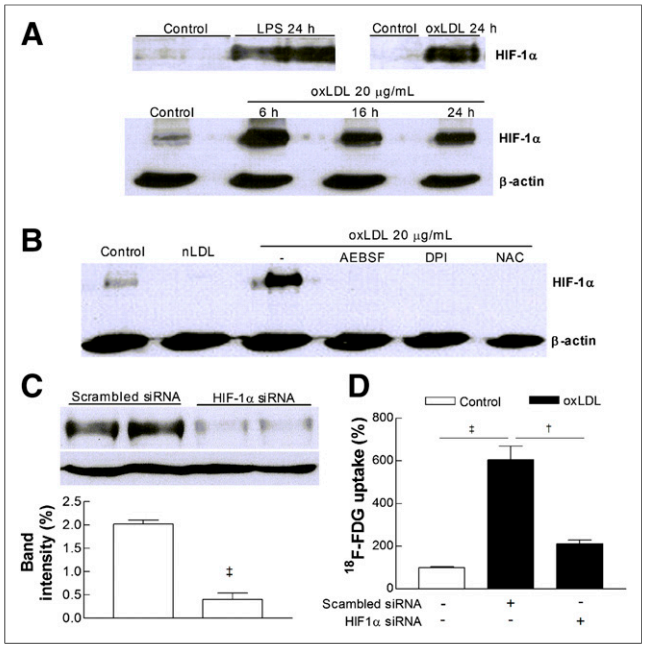

FIGURE 5. oxLDL promotes macrophage HIF-1α accumulation through ROS generation. (A) HIF-1α levels in RAW264.7 cells exposed to 100 ng of lipopolysaccharide per milliliter or 20 μg of oxLDL per milliliter for 24 h (top) and time course of HIF-1α accumulation (bottom). (B) Effects of DPI (1 μM), AEBSF (0.3 mM), and NAC (10 mM) on HIF-1α accumulation stimulated by 24-h treatment with 20 μg of oxLDL per milliliter. (C) HIF-1α level in cells transduced with scrambled siRNA or HIF-1α–specific siRNA. Bars are mean ± SEM of data from 2 independent experiments (n = 4). (D) Effects of scrambled siRNA or HIF-1α siRNA on oxLDL-stimulated ^{18}F-FDG uptake. Bars are mean ± SEM of data from 2 independent experiments (n = 6) expressed as percentage uptake relative to controls. LPS = lipopolysaccharide.

Taken together, these findings indicate that Nox2 is likely responsible for the observed metabolic effects of oxLDL on RAW264.7 cells.

Atherosclerotic plaques are often characterized by poor vascularization, requiring recruited macrophages to survive and perform physiologic functions under a hypoxic environment (*17*). Cell responses to low oxygen are mediated by HIF-1α, a key orchestrator of genes necessary for hypoxic adaptation (*34*). HIF-1α–mediated responses including enhanced glycolysis can promote macrophage survival under hypoxic stress (*18*) and are also necessary for inflammatory response mediation (*19*). In our study, normoxic RAW264.7 cells showed a low level of baseline HIF-1α expression, a finding that has also been observed in previous studies (*35*). Although hypoxia is the major stimulant for HIF-1α expression, other diverse agonists have been identified to stabilize HIF-1α in normoxic macrophages (*36*), possibly indicating a potential role of HIF-1α in coordinating basal macrophage function. The baseline HIF-1α expression appeared to be suppressed by nLDL, which was an unexpected finding given the poor expression of nLDL receptors in differentiated macrophages and the inability of nLDL to induce foam cell formation under usual conditions (*37*). Hence, the mechanism of this finding is not clear and may require further investigation for clarification. When normoxic RAW264.7 cells were treated with oxLDL, this substantially promoted HIF-1α accumulation. Moreover, silencing of HIF-1α expression with siRNA completely abrogated the ability of oxLDL to augment ^{18}F-FDG uptake, demonstrating that HIF-1α activation is essential for oxLDL-induced stimulation of glycolytic flux in macrophages. Furthermore, the increase of HIF-1α accumulation and heightened ^{18}F-FDG uptake induced by oxLDL were both completely blocked by ROS scavenging with NAC, as well as by inhibition of NADPH oxidase activity with AEBSF or DPI. ROS has been suggested to be able to suppress the proteolytic degradation of HIF-1α by inhibiting prolyl hydroxylase activity. Our results support the dependence on a ROS-sensitive pathway of increased HIF-1α accumulation and ^{18}F-FDG uptake by oxLDL (Fig. 6).

A limitation of our study is that although we confirmed oxLDL-stimulated ^{18}F-FDG uptake in multiple types of macrophages including murine peritoneal and human peripheral monocyte/macrophages, other experiments were performed only on RAW264.7 cells. Because the metabolic characteristics of proliferating macrophage cell lines can be different from harvested macrophages and species-specific differences may also be present, key findings of our study may need to be confirmed with harvested human macrophages.

CONCLUSION

Our results demonstrate that exposure to oxLDL significantly increases RAW264.7 macrophage ^{18}F-FDG uptake and glycolytic metabolism through upregulation of GLUT1 expression and hexokinase activity. This response is mediated by HIF-1α activation, which in turn is dependent on augmented ROS generation induced by increased Nox2 expression.

DISCLOSURE

The costs of publication of this article were defrayed in part by the payment of page charges. Therefore, and solely to indicate this fact, this article is hereby marked "advertisement" in accordance with 18 USC section 1734. This work was supported by Samsung Biomedical Research Institute grant # SMX1131891 and the New Faculty Research Fund at the Ajou University School of Medicine. No other potential conflict of interest relevant to this article was reported.

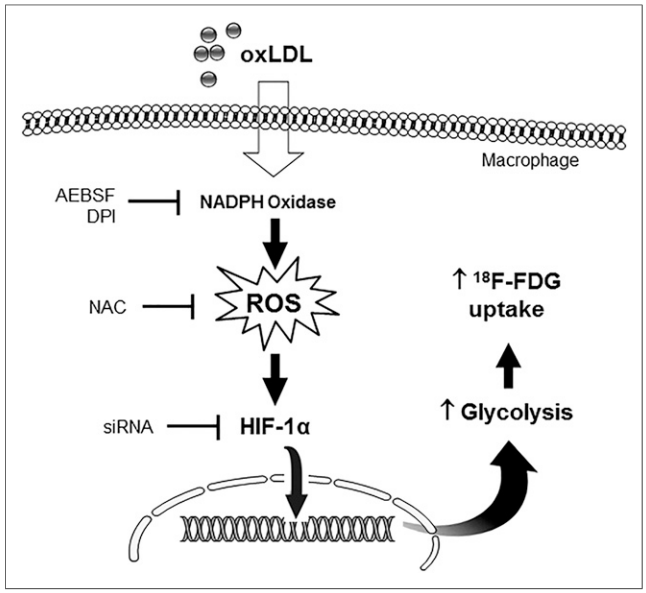

FIGURE 6. Schematic representation of intracellular molecular mechanisms leading to increased ^{18}F-FDG uptake and enhanced glycolysis in macrophages stimulated with oxLDL. LPS = lipopolysaccharide.

REFERENCES

1. Hansson GK. Inflammation, atherosclerosis, and coronary artery disease. *N Engl J Med.* 2005;352:1685–1695.
2. Rudd JH, Warburton EA, Fryer TD, et al. Imaging atherosclerotic plaque inflammation with [^{18}F]-fluorodeoxyglucose positron emission tomography. *Circulation.* 2002;105:2708–2711.
3. Noh TS, Moon SH, Cho YS, et al. Relation of carotid artery ^{18}F-FDG uptake to C-reactive protein and Framingham risk score in a large cohort of asymptomatic adults. *J Nucl Med.* 2013;54:2070–2076.
4. Rominger A, Saam T, Wolpers S, et al. ^{18}F-FDG PET/CT identifies patients at risk for future vascular events in an otherwise asymptomatic cohort with neoplastic disease. *J Nucl Med.* 2009;50:1611–1620.
5. Lee SJ, On YK, Lee EJ, Choi JY, Kim BT, Lee KH. Reversal of vascular ^{18}F-FDG uptake with plasma high-density lipoprotein elevation by atherogenic risk reduction. *J Nucl Med.* 2008;49:1277–1282.
6. Tahara N, Kai H, Ishibashi M, et al. Simvastatin attenuates plaque inflammation: evaluation by fluorodeoxyglucose positron emission tomography. *J Am Coll Cardiol.* 2006;48:1825–1831.
7. Gleissner CA, Leitinger N, Ley K. Effects of native and modified low-density lipoproteins on monocyte recruitment in atherosclerosis. *Hypertension.* 2007; 50:276–283.
8. Hundal RS, Gomez-Munoz A, Kong JY, et al. Oxidized low density lipoprotein inhibits macrophage apoptosis by blocking ceramide generation, thereby maintaining protein kinase B activation and Bcl-XL levels. *J Biol Chem.* 2003; 278:24399–24408.
9. Stocker R, Keaney JF Jr. Role of oxidative modifications in atherosclerosis. *Physiol Rev.* 2004;84:1381–1478.
10. Kim C, Kim S. Taurine chloramine inhibits LPS-induced glucose uptake and glucose transporter 1 expression in RAW 264.7 macropages. *Adv Exp Med Biol.* 2009;643:473–480.
11. Paik JY, Lee KH, Choe YS, Choi Y, Kim BT. Augmented ^{18}F-FDG uptake in activated monocytes occurs during the priming process and involves tyrosine kinases and protein kinase C. *J Nucl Med.* 2004;45:124–128.
12. Tavakoli S, Zamora D, Ullevig S, Asmis R. Bioenergetic profiles diverge during macrophage polarization: implications for the interpretation of ^{18}F-FDG PET imaging of atherosclerosis. *J Nucl Med.* 2013;54:1661–1667.
13. De Vries HE, Ronken E, Reinders JH, Buchner B, Van Berkel TJ, Kuiper J. Acute effects of oxidized low density lipoprotein on metabolic responses in macrophages. *FASEB J.* 1998;12:111–118.
14. Ogawa M, Nakamura S, Saito Y, Kosugi M, Magata Y. What can be seen by ^{18}F-FDG PET in atherosclerosis imaging? The effect of foam cell formation on ^{18}F-FDG uptake to macrophages in vitro. *J Nucl Med.* 2012;53:55–58.
15. Elsegood CL, Chang M, Jessup W, Scholz GM, Hamilton JA. Glucose metabolism is required for oxidized LDL-induced macrophage survival: role of PI3K and Bcl-2 family proteins. *Arterioscler Thromb Vasc Biol.* 2009;29:1283–1289.
16. Folco EJ, Sheikine Y, Rocha VZ, et al. Hypoxia but not inflammation augments glucose uptake in human macrophages: implications for imaging atherosclerosis with ^{18}fluorine-labeled 2-deoxy-D-glucose positron emission tomography. *J Am Coll Cardiol.* 2011;58:603–614.
17. Lewis JS, Lee JA, Underwood JC, Harris AL, Lewis CE. Macrophage responses to hypoxia: relevance to disease mechanisms. *J Leukoc Biol.* 1999;66:889–900.
18. Roiniotis J, Dinh H, Masendycz P, et al. Hypoxia prolongs monocyte/macrophage survival and enhanced glycolysis is associated with their maturation under aerobic conditions. *J Immunol.* 2009;182:7974–7981.
19. Cramer T, Yamanishi Y, Clausen B, et al. HIF-1α is essential for myeloid cell-mediated inflammation. *Cell.* 2003;112:645–657.
20. Rodríguez-Prados JC, Través PG, Cuenca J, et al. Substrate fate in activated macrophages: a comparison between innate, classic, and alternative activation. *J Immunol.* 2010;185:605–614.
21. Bae YS, Lee JH, Choi SH, et al. Macrophages generate reactive oxygen species in response to minimally oxidized low-density lipoprotein: toll-like receptor 4- and spleen tyrosine kinase-dependent activation of NADPH oxidase 2. *Circ Res.* 2009;104:210–218.
22. Brunelle JK, Bell EL, Quesada NM, et al. Oxygen sensing requires mitochondrial ROS but not oxidative phosphorylation. *Cell Metab.* 2005;1:409–414.
23. Mansfield KD, Guzy RD, Pan Y, et al. Mitochondrial dysfunction resulting from loss of cytochrome c impairs cellular oxygen sensing and hypoxic HIF-alpha activation. *Cell Metab.* 2005;1:393–399.
24. Bonello S, Zähringer C, BelAiba RS, et al. Reactive oxygen species activate the HIF-1α promoter via a functional NFkappaB site. *Arterioscler Thromb Vasc Biol.* 2007;27:755–761.
25. Nishi K, Oda T, Takabuchi S, et al. LPS induces hypoxia-inducible factor 1 activation in macrophage-differentiated cells in a reactive oxygen species-dependent manner. *Antioxid Redox Signal.* 2008;10:983–995.
26. Shatrov VA, Sumbayev VV, Zhou J, Brüne B. Oxidized low-density lipoprotein (oxLDL) triggers hypoxia-inducible factor-1α (HIF-1α) accumulation via redox-dependent mechanisms. *Blood.* 2003;101:4847–4849.
27. Fu Y, Maianu L, Melbert BR, Garvey WT. Facilitative glucose transporter gene expression in human lymphocytes, monocytes, and macrophages: a role for GLUT isoforms 1, 3, and 5 in the immune response and foam cell formation. *Blood Cells Mol Dis.* 2004;32:182–190.
28. Byeon SE, Yi YS, Oh J, Yoo BC, Hong S, Cho JY. The role of Src kinase in macrophage-mediated inflammatory responses. *Mediators Inflamm.* 2012;2012: 512926.
29. Fougerat A, Gayral S, Malet N, Briand-Mesange F, Breton-Douillon M, Laffargue M. Phosphoinositide 3-kinases and their role in inflammation: potential clinical targets in atherosclerosis? *Clin Sci (Lond).* 2009;116:791–804.
30. Forman HJ, Torres M. Reactive oxygen species and cell signaling: respiratory burst in macrophage signaling. *Am J Respir Crit Care Med.* 2002;166:S4–S8.
31. Fischer B, von Knethen A, Brüne B. Dualism of oxidized lipoproteins in provoking and attenuating the oxidative burst in macrophages: role of peroxisome proliferator-activated receptor-gamma. *J Immunol.* 2002;168:2828–2834.
32. Lee CF, Qiao M, Schröder K, Zhao Q, Asmis R. Nox4 is a novel inducible source of reactive oxygen species in monocytes and macrophages and mediates oxidized low density lipoprotein-induced macrophage death. *Circ Res.* 2010;106:1489–1497.
33. Sasaki H, Yamamoto H, Tominaga K, et al. NADPH oxidase-derived reactive oxygen species are essential for differentiation of a mouse macrophage cell line (RAW264.7) into osteoclasts. *J Med Invest.* 2009;56:33–41.
34. Denko NC. Hypoxia, HIF1 and glucose metabolism in the solid tumour. *Nat Rev Cancer.* 2008;8:705–713.
35. Anand RJ, Gribar SC, Li J, et al. Hypoxia causes an increase in phagocytosis by macrophages in a HIF-1α-dependent manner. *J Leukoc Biol.* 2007;82:1257–1265.
36. Zhou J, Fandrey J, Schümann J, Tiegs G, Brüne B. NO and TNF-α released from activated macrophages stabilize HIF-1α in resting tubular LLC-PK1 cells. *Am J Physiol Cell Physiol.* 2003;284:C439–C446.
37. Kruth HS, Huang W, Ishii I, Zhang WY. Macrophage foam cell formation with native low density lipoprotein. *J Biol Chem.* 2002;277:34573–34580.

The Journal of NUCLEAR MEDICINE

Oxidized Low-Density Lipoprotein Stimulates Macrophage ^{18}F-FDG Uptake via Hypoxia-Inducible Factor-1 α Activation Through Nox2-Dependent Reactive Oxygen Species Generation

Su Jin Lee, Cung Hoa Thien Quach, Kyung-Ho Jung, Jin-Young Paik, Jin Hee Lee, Jin Won Park and Kyung-Han Lee

J Nucl Med. 2014;55:1699-1705.
Published online: September 11, 2014.
Doi: 10.2967/jnumed.114.139428

The Journal of Nuclear Medicine is published monthly.
SNMMI | Society of Nuclear Medicine and Molecular Imaging
1850 Samuel Morse Drive, Reston, VA 20190.
(Print ISSN: 0161-5505, Online ISSN: 2159-662X)

SNMMI SOCIETY OF NUCLEAR MEDICINE AND MOLECULAR IMAGING